Performance of piezoelectric patch actuators for vibration control of honeycomb panels

Corine Florens[1]**, Etienne Balmes**[1,2]

[1]Ecole Centrale Paris, MSSMat, 92295 Chatenay Malabry, France

[2]SDTools, 44 Rue Vergniaud, 75013 Paris, France

balmes@sdtools.com

Abstract

Active control has often been considered for low frequency noise control of aircraft or helicopter trim panels. In the case of honeycomb panels results were not always as good as expected. To gain a better understanding the present study introduces a detailed model of a honeycomb beam equipped with piezoelectric patches. A first result is the experimental validation of the model. From this test a clear understanding of local skin bending is achieved. This effect induces poor coupling of the patch with low frequency modes, and thus limits the achievable performance for active control. Finally modeling strategies for the integration of the model in a numerical design process are discussed.

Keywords : **active control/ honeycomb/ test-analysis correlation**

Le contrôle actif à souvent été considéré pour la maitrise du bruit basse fréquence des panneaux d'habillage des avions et hélicoptères. Dans le cas de panneaux en nid d'abeille, les résultats n'ont pas toujours été à la hauteur des attentes. L'étude présentée introduit un modèle détaillé de panneau en nid d'abeille équipé de patchs piézoélectriques. Un premier résultat est la validation expérimentale de ce modèle. Cette validation donne une compréhension claire des effets locaux présents dans les peaux. Ces effets correspondent à un faible couplage entre les patchs et les modes basses fréquences. La performance atteignable par le contrôle actif est donc limitée. Finalement, des stratégies pour l'intégration du modèle proposé dans un processus de conception sont discutées.

Mots clés : **contrôle actif/ nid d'abeille/ corrélation calcul-essai**

1   Introduction

Reduction of noise transmission inside cabins, for improved passenger comfort, is an important concern for the aircraft industry. Usually trim panels are made of honeycomb sandwich composite. Those panels have a high strength to weight ratio, but acoustical properties have to be improved by complementary treatments. Passive treatments are efficient for high frequencies. Active sound and vibration control is a solution to reduce residual noise for low and medium frequencies.

While active control of honeycomb panels has been the object of various studies [1, 2], detailed modeling of the panels equipped with piezoelectric patches was not performed. In general, such modeling seems necessary to achieve a consistent design methodology. In the present study, the observation of local bending effects in the honeycomb skin is shown to be a factor limiting the performance and thus clearly confirms the need for modeling to guide design refinement.

Section 2 summarizes the constitutive model used to represent the honeycomb equipped with patches. The honeycomb is modeled as an assembly of three models : two skins, modeled as composite plates, and a core,

modeled as an equivalent orthotropic material. The extension of the composite plate model to account for piezoelectric coupling in the patches is then shown. Finally, the strategy for solving equations is discussed.

Section 3 details the experimental validation of the proposed model. In particular, the high level of skin bending effects present in the residual flexibility is validated in detail.

Finally section 4 discusses practical constraints linked to the use of the proposed model in a design phase.

2 Model formulation

2.1 Constitutive model of the panel

When modeling honeycomb panels, the use of detailed 3D models where each of the walls of the honeycomb is modeled can rapidly become inaccessible. The classical approach is thus to build an equivalent model with skins modeled as shells and the honeycomb modeled using an orthotropic material. A wide range of equivalent formulas giving the orthotropic material properties as function of the cell properties can be found in the literature [3, 4, 5, 6].

The results shown here are based on the methodology introduced in [7]. The principle of this approach is to compare the frequencies of modes obtained with periodicity conditions that are equivalent for both models shown in figure 1.
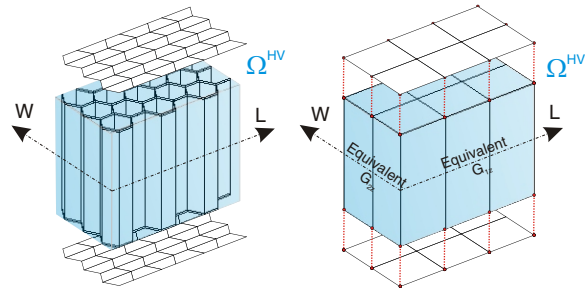

Figure 1: Homogenized Volume considered.

The piezoelectric plate element, implemented in [8] and considered in this work, is based on Classical Laminated Plate Theory (CLPT [9, 10]) for the mechanical part and the work of Piefort [11] for the piezoelectric coupling.
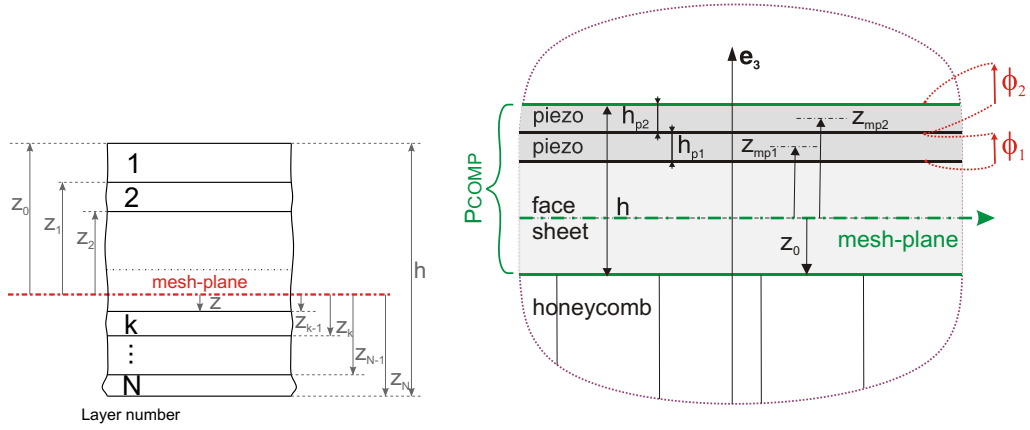
Figure 2: **Left** Geometry of an N-layered laminate. **Right** Particularization for a skin with a piezoelectric patch

The global constitutive equations of piezoelectric Mindlin shell are obtained by integration over thickness and are expressed in the global coordination system. The piezoelectric medium has orthotropic mechanic and electric properties; hence the constitutive equations for each layer are related to their orthotropic axes. $[R_T]_k^{-1}$ is the transformation matrixes linking the stresses in the local coordinate system to the global one, and $[R_S]_k$ that linking the strain in the global coordinate system to the local one. The coupled plate/piezoelectric equations are thus given by

$$
\left\{\begin{array}{c} N \\ M \\ Q \\ \vdots \\ D_k \\ \vdots \end{array}\right\} = \left[\begin{array}{ccc|ccc} A & B & 0 & \cdots & ([e]_k\,[R_s^k])^T & \cdots \\ B & D & 0 & \cdots & (z_{mk}[e]_k\,[R_s^k])^T & \cdots \\ 0 & 0 & H & \cdots & 0 & \cdots \\ \hline \vdots & \vdots & \vdots & \ddots & & 0 \\ [e]_k\,[R_s^k] & z_{mk}\,[e]_k\,[R_s^k] & 0 & & -\frac{\epsilon_k}{h_k} & \\ \vdots & \vdots & \vdots & 0 & & \ddots \end{array}\right] \left\{\begin{array}{c} S^m \\ \kappa \\ \gamma \\ \vdots \\ \phi_k \\ \vdots \end{array}\right\} \tag{1}
$$

where the matrix $[A], [B], [D]$, are respectively the extensional stiffness matrix, the extension/bending coupling matrix, and the bending stiffness matrix, classical stiffness matrix for a composite laminate (see [9]).

It is assumed that the electric field needs only to be known between electrodes and can be described by the difference of potential ϕ_k, leading to an assumed electric field $\vec{E} = -\vec{grad}\phi$. When this field is applied in the direction $\vec{e}_3$, the piezoelectric actuator PZT extends in the plane $(\vec{e}_1, \vec{e}_2)$. It produces load on the piezoelectric layer (or ply in the CLPT terminology) in the direction $\vec{e}_1$ which depends on e_{31} and ϕ. Because of the offset between the mid-plane of the actuator and the mi-plane of the multilayer laminate, the force induces both membrane and bending loads as will be illustrated in section 3.

In the software implementation, the composite plate is modeled using a classical MITC4 element [12]. The piezoelectric coupling part of (1) is numerically integrated using the nominal four point rule on the patch. For the electric part, a single electric DOF is considered for each patch. This DOF is thus common to all elements covered by the electrode. In the present configuration two patches are stacked together thus leading to a model with two electric DOFs. In practice, the wiring is such that these potential are equal or opposite. The elimination of this constraint is done in the model resolution phase.

2.2 Resolution of system equations

Once assembled the model takes the form

$$\begin{bmatrix} Z_{uu} & K_{u\phi} \\ K_{\phi u} & K_{\phi\phi} \end{bmatrix} \begin{Bmatrix} q_{mech} \\ \phi_k \end{Bmatrix} = \begin{Bmatrix} F_{mech} \\ Q_k \end{Bmatrix} \tag{2}$$

with the classical dynamic stiffness $Z = Ms^2 + K$.

When simulating the response, one needs to consider sensor and actuator configurations.

Piezoelectric patches used as sensors have a charge that remains zero (open circuit mode). One can thus condense the electric DOF. Indeed, one considers an electrostatic behavior (no $M_{\phi\phi}$ or $M_{\phi u}$) and assumes $Q_k = 0$, one thus has

$$\begin{Bmatrix} \{q_{mech}\} \\ \phi_k \end{Bmatrix} = \begin{bmatrix} I \\ -[K_{\phi\phi}]^{-1}[K_{\phi u}] \end{bmatrix} \{q\}_{mech} = [T]\{q_{mech}\} \tag{3}$$

This relation can be used to eliminate the electric contribution from the system equations which become

$$[T]^T[Z][T]\{q_{mech}\} = [T]^T\{F\} \tag{4}$$

From this condensation it clearly appears that a patch used as sensor induces a shift of frequencies form a configuration without piezoelectric coupling.

Piezoelectric patches used as actuators have a difference of potential ϕ_k that is enforced. One can thus use the electric part of (2) to determine the charge

$$Q_k = [K_{\phi u} \ K_{\phi\phi}] \begin{Bmatrix} q_{mech} \\ \phi_k \end{Bmatrix} \tag{5}$$

and consider the system equations with no piezoelectric coupling and an electric load

$$Z_{uu}q_{mech} = F_{mech} - K_{u\phi}\phi_k \tag{6}$$

It clearly appears that the dynamic stiffness of this configuration is that of the purely mechanical model with no piezoelectric coupling. The modes of Z_{uu} correspond to the case with ϕ_k set to zero. In other words, the actuator configuration leads to closed circuit modes.

In the resolution process implemented in [8], electrodes are declared to be either open or closed circuit which allows a condensation or elimination of electrical DOFs before computation of modes and static correction for inputs [13], which are used to build the state-space model. The inclusion of the static correction is shown to be critical in the next section.

3 Experimental validation

Experimental validation was performed using piezo and laser vibrometer measurements. In a first campaign performed at the Marcus Wallenberg Laboratory for Sound and Vibration Research (MWL) of KTH Stockholm University, shown in figure 3, measurements over the full length of the beam were performed to obtain global modeshapes correlation. When local effects were shown, a second test was performed at Ecole Centrale Paris, using a dense mesh of measurement points located over the patch.
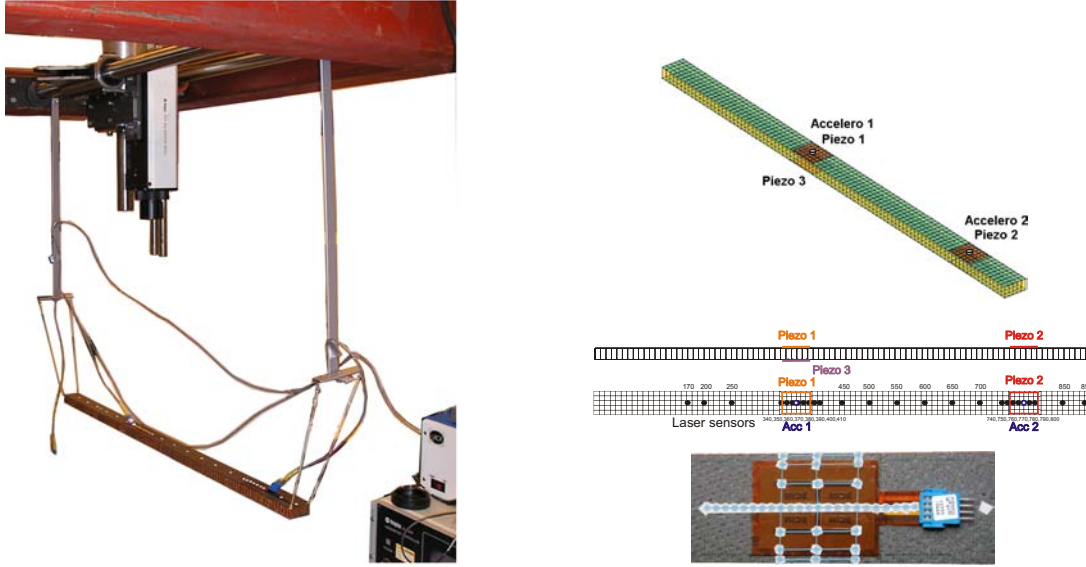
Figure 3: Experimental Setup. Left : full beam measurements. Top right, piezo patch configuration. Bottom right : sensor location of zoom on patch

The test beam external dimensions are $900 \times 45 \times 21mm$. The skins are 1 mm carbon laminates. The core is a 19 mm thick Nomex paper honeycomb. Initial test of the beam properties are detailed in Ref. [7]. As shown ther, Nomex based honeycomb and/or glue have viscoelastic behavior, i.e. a frequency dependent behavior. Figure 4 demonstrates that excellent test/analysis correlation is achieved, provided that the frequency dependence of the honeycomb properties is taken into account.
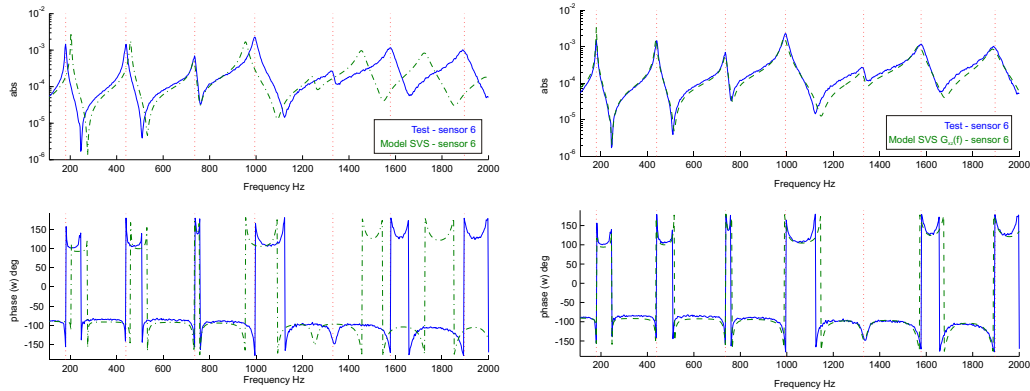

Figure 4: Piezo voltage to translation transfer on a carbon/nomex honeycomb beam (Piezo 1 actuator - Laser sensor 6). **Left** : Elastic model. **Right** viscoelastic model.

One of the key results of the experiment was a clear understanding of the limitations of the actuation mechanism obtained by placing patches on the skin. The problematic shape is illustrated by simulation results shown in figure 5.

It is well known that patches generate loads that correspond to a combination of in plane membrane traction and moments applied on the edges. The use of a two layer patch in the QuickPack is meant to allow users select a preferred actuation mechanism depending on whether the two applied voltages ϕ_1, ϕ_2 have equal or opposite polarity. In the considered setup, the polarity favoring membrane loading is used. The objective is to generate an elongation of the skin and thus a global bending of the beam.

The shape, shown in figure 5, clearly indicates a poor actuation mechanism. While bending of the overall beam is achieved, the dominant effect at this frequency is a very local bending of the skin. The effect is even large enough to generate a local bending of the opposite skin.
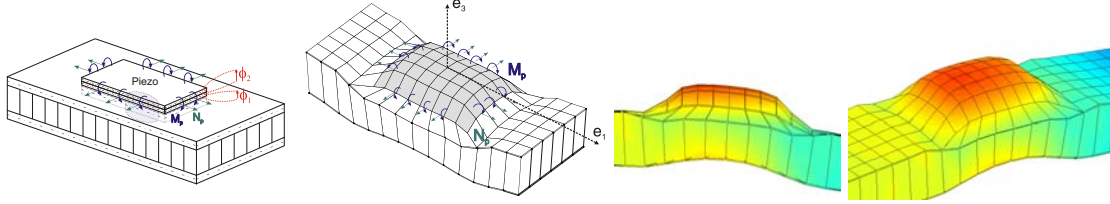

Figure 5: Blister of piezoelectric actuator obtained by simulation.

With such behavior, the patch is more effective as a local loudspeaker than as a actuator on global bending modes. The result being far from obvious and not documented in the literature, detailed tests were performed.

First, it is important to understand that the localized bending effect cannot be seen in the shape of the low frequency modes. To illustrate the point, figures 6 and 7 compare forced responses, computed and simulated at and around the second mode resonance.

The test/analysis correlation is very good and clearly demonstrates that the modeshape does not show the blister shape while off-resonance responses show it extremely clearly. This illustrates experimentally the effect of residual flexibility. The blister shape is the deformation generated by the application of a static voltage on the patch. For vibration applications, the response is a linear combination of the modal contributions and a quasi-static effect, often called residual flexibility [14]. This test illustrates the fact that the residual flexibility induces a major local effect. This effect has an obvious limiting effect on the ability to control noise radiated by the panel since control of the modes will generate a local noise source even on the skin opposite to the patch.
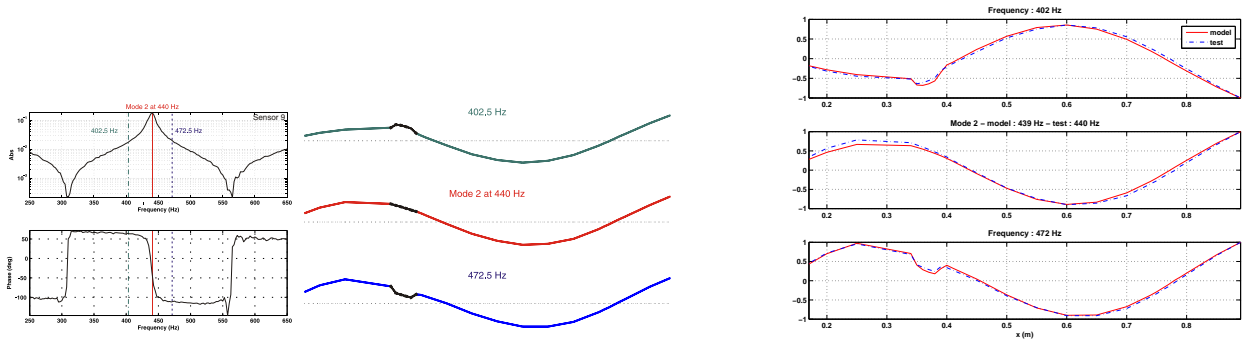

Figure 6: Second test mode of the carbon/nomex honeycomb core beam actuated by the piezoelectric patch 1 in the middle of the patch - Shape before, at, and after resonance. Test analysis/correlation.
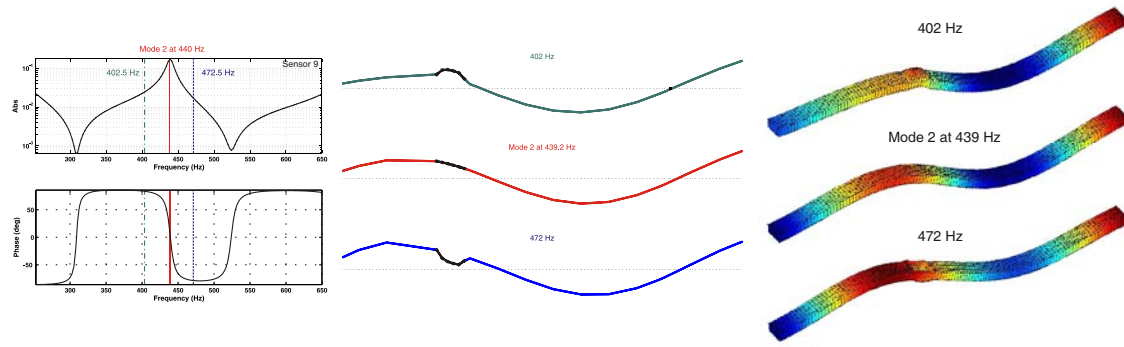
Figure 7: Second mode of the carbon/nomex honeycomb core beam actuated by the piezoelectric patch 1 in the middle of the patch obtained by numerical simulation - Shape before, at, and after resonance.

To establish the test/analysis correlation more firmly, the density of measurements was strongly refined on the patch in both x and y directions. The quantitative comparison of the local patch deflection in x and y directions are presented in figure 8. Measurement errors are visible, especially in x direction because the sensors were really close, only 3.8 mm between each reflector. Despite the measurement error, the shapes are clearly extremely well correlated. The FE model presented is thus clearly validated.
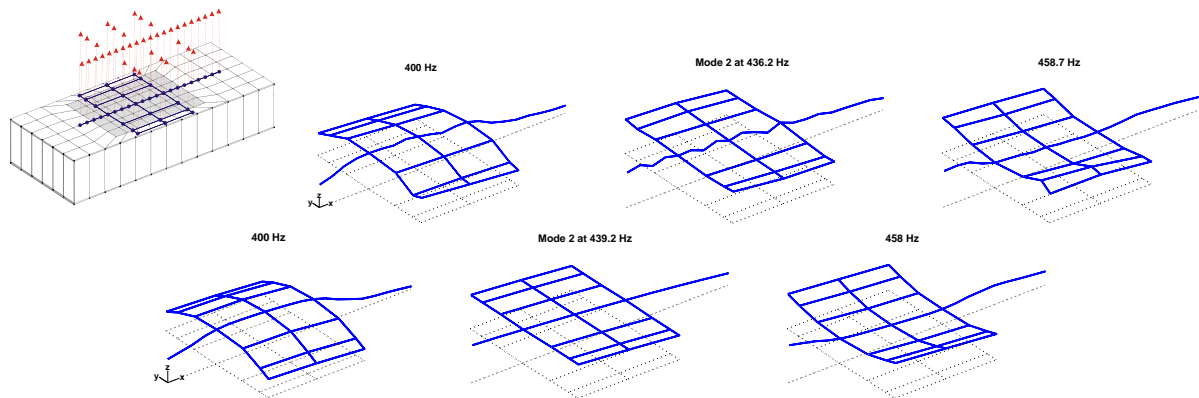

Figure 8: Test (**top**) and simulation (**bottom**): before resonance at 400Hz, at resonance, and after resonance at 458Hz.

4   Strategies for integrating piezos into FE models

Having validated a model, this section focuses on the practical implementation of the modeling strategy. The model considered in previous sections implies significant adaptations. As shown in 9/a, the mesh is adapted in the vicinity of the patch and two composite properties are considered. One for the standard honeycomb skin (shown in blue in the figure) and one for the patch which includes multiple layers for the skin plus two layers for the patch, as shown in figure 2.

This approach is fine for a small beam model and if only few configurations of patch locations are considered. Indeed, the adaptation of the mesh under the patches would be quite time consuming for a large panel where multiple patch configurations would need to be tested. Furthermore, the use of viscoelastic materials in the glue, considered by many in the literature, would imply the use of a volume layer for the glue.

The idea tested in this work is thus to use separate elements to model the skin and the piezoelectric patch, with linear constraints used to account for the offset between the two. The shear stiffness of the glue layer

(G/h) is deemed sufficiently high to suppose perfect bonding and thus omit glue modeling.

An automated procedure was introduced to mesh the patch. Based on a given rectangular shape, skin elements strictly under the patch are projected to the patch mid-surface. The boundary between the projected elements and the edge of the reference rectangle is then meshed automatically. The resulting model is shown in figure 9/c. This approach is deemed more acceptable than an adaptation of the honeycomb mesh because it only affects a small part of the model and would be adapted for the reuse of modes of the nominal panel.

As an intermediate validation, a model with two layers (skin and piezo) but an adapted underlying mesh is also considered and shown in 9/b.
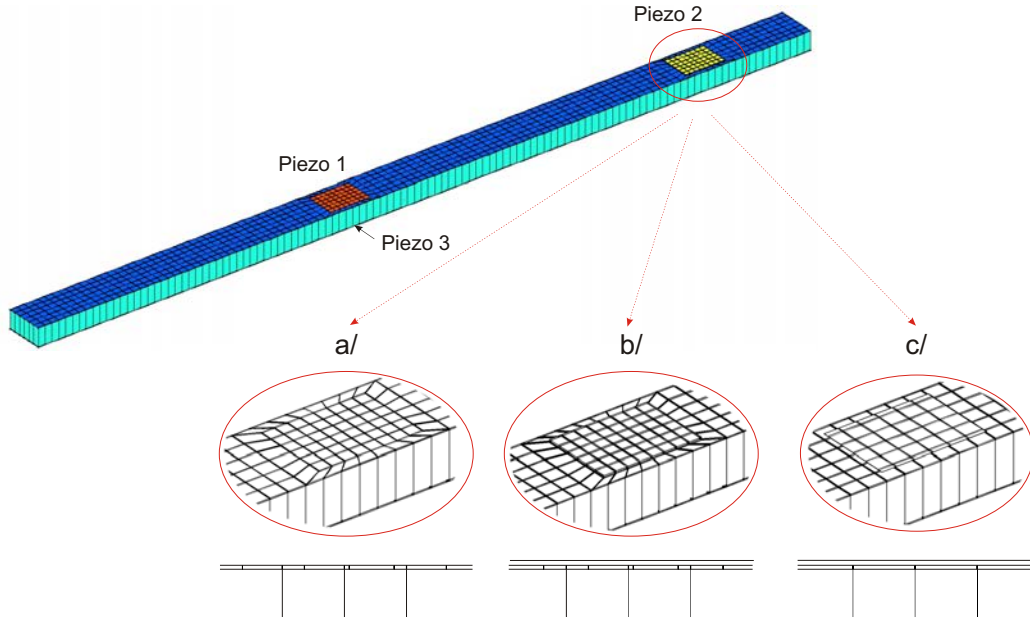

Figure 9: Piezoelectric patch model strategy: a/ adapted meshing and integrated patch, b/ adapted meshing and 2 layers (patch and face sheet), c/ non-adapted meshing and 2 layers.

To compare these models, electric transfers are shown in figure 10 and piezo to laser transfers in figure 11. For a cross transfer from voltage input on piezo 2 to voltage output on piezo 1, the responses are almost perfectly superposed. For the impedance $\frac{Q_{Piezo2}}{V_{Piezo2}}$ however, there is a significant offset of about 30 % on the static response. This error can reasonably be attributed to the lack of adaptation of the mesh on the patch edges. This is illustrated in figure 12 which shows the quasistatic shaped generated by the actuation (since the structure is free floating, one shows the deformation at 1 Hz which avoids problems linked to rigid body modes). The deformations clearly show that the blister shape under the patch cannot be perfectly reproduced due to the lack of mesh adaptation.

The proposed strategy using multiple-elements through the thickness is thus limited by the ability to reproduce local effects under the patch. The local nature of this effect is clearly considered a design flaw of the considered configuration. With better designs, the patch would induce bending with much greater wave length and the mesh adaptation would probably be not as necessary.
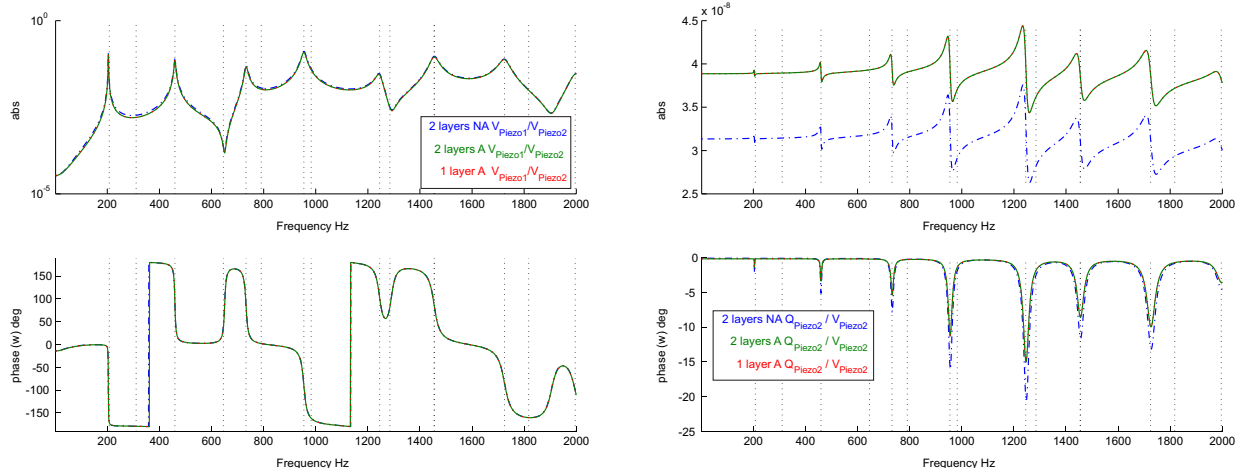
Figure 10: Electric transfers for the 3 model strategies. Input is piezo 2 used as voltage driven actuator. **Left** piezo 1 used as voltage sensor. **Right** Charge generated on piezo 2.
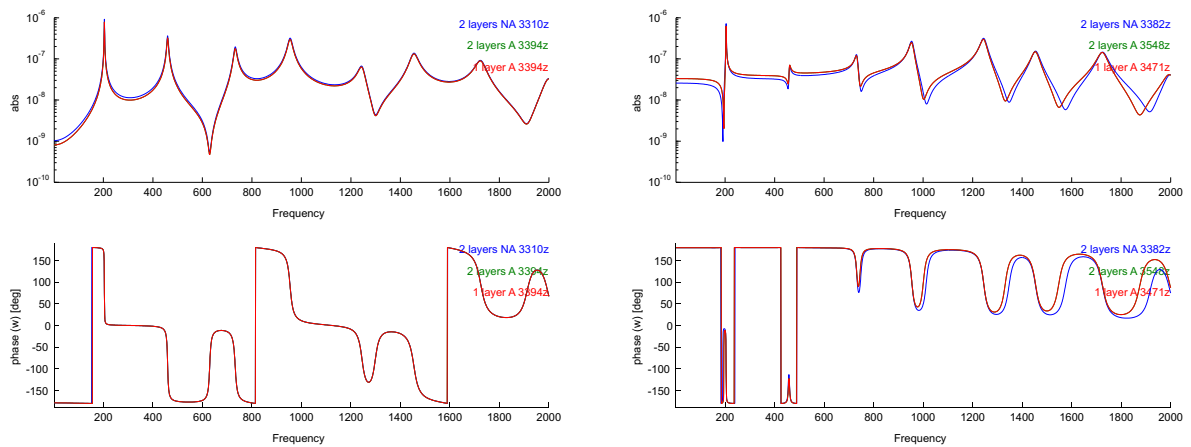

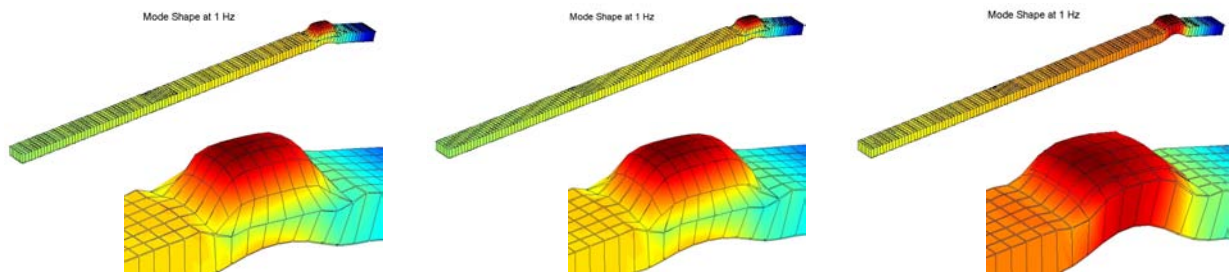Figure 11: Piezo to laser sensor transfer .

Figure 12: Shape at 1Hz for the 3 model strategies of the piezoelectric actuator (Piezo2).

5 Conclusion

Modeling techniques for honeycomb panels equipped with piezoelectric patches are very well correlated with experiments. The particular configuration studied shows very strong local effects in the skins, which would give poor results for applications in an active control experiment. The authors believe that a complete redesign of the actuator is necessary to achieve good performance in such configurations.

References

[1] Bihan, D. L., Lepage, A., Florens, C., and Roudolff, F., "Contrôle Actif de panneaux composites," *Technical Report RT 1/08836 DDSS*, April 2005.

[2] Lepage, A., Mortain, F., and Coste, L., "Active Structural Acoustic Control of a Helicopter Trim Panel," *INTERNOISE 2005, Rio de Janeiro, Brazil*, August 2005.

[3] Gibson, L. J. and Ashby, M. F., *Cellular Solids Structure and Properties, Second Edition*, Cambridge University Press, 1997.

[4] Grédiac, M., "A finite element study of the transverse shear in honeycomb cores," *International Journal of Solids and Structures*, Vol. 30(13), 1993, pp. 1777–1788.

[5] Noor, A. and Burton, W., "Assessment of continuum models for sandwich panel honeycomb cores," *Computer methods in applied mechanics and engineering*, Vol. 145, 1997, pp. 341–360.

[6] Hohe, J. and Becker, W., "A refined analysis of the effective elasticity tensor for general cellular sandwich cores," *International Journal of Solids and Structures*, Vol. 38, 2001, pp. 3689–3717.

[7] Florens, C., Balmes, E., Clero, F., and Corus, M., "Accounting for glue and temperature effects in Nomex based honeycomb models," *ISMA*, September 2006.

[8] Balmes, E., Leclère, J., and Bianchi, J., *Structural Dynamics Toolbox 6.0 (for use with MATLAB)*, SDTools, Paris, France, www.sdtools.com, May 2007.

[9] Jones, R. M., *Mechanics of Composite Materials*, Hemisphere Publishing Corp., 1975.

[10] Berthelot, J.-M., *Materiaux composites - Comportement mecanique et analyse des structures*, Masson, 1992.

[11] Piefort, V., *Finite Element Modelling of Piezoelectric Active Structures*, Ph.D. thesis, Active Structures Laboratory Department of Mechanical Engineering and Robotics, Université Libre de Bruxelles, Belgium., 2001.

[12] Bathe, K. and Chapelle, D., *The finite element analysis of shells – fundamentals*, Springer, 2003.

[13] Balmes, E., *Methods for vibration design and validation*, Course notes Ecole Centrale Paris, 1997-2007.

[14] Craig, R. J., "A Review of Time-Domain and Frequency Domain Component Mode Synthesis Methods," *Int. J. Anal. and Exp. Modal Analysis*, Vol. 2, No. 2, 1987, pp. 59–72.